STM JOURNALS

Journal of
Polymer & Composites

ISSN: 2321-2810 (Online)
ISSN: 2321-8525 (Print)
Volume 13, Issue 6, 2025
DOI (Journal): 10.37591/JoPC

https://journals.stmjournals.com/jopc/

Research JoPC

Experimental Study on the Impact of Polymer (PAM) in Enhancing Oil Recovery in Upper Assam Basin Oil fields

Joyshree Barman[1], Bhaskar Jyoti Saikia[2,*], Ranjan Phukan[3], Gauri Sankar Bora[4]

Abstract

The Upper Assam Basin, one of India's most mature and extensively exploited hydrocarbon provinces, is experiencing declining oil production due to reservoir depletion and unfavorable crude oil–brine–rock (COBR) interactions. In this context, alkali–polymer (AP) flooding has emerged as a promising chemical enhanced oil recovery (EOR) strategy. AP flooding reduces interfacial tension (IFT) through in-situ surfactant generation by alkali and improves sweep efficiency via polymer-based mobility control, typically using polyacrylamide (PAM). This study evaluates the feasibility and performance of AP flooding in representative sandstone cores from the basin through laboratory experiments and numerical simulation. Rheological characterization using a coaxial cylinder viscometer confirmed that PAM exhibits shear-thinning behavior at higher concentrations, favorable for mobility control in heterogeneous reservoirs. Coreflooding experiments demonstrated encouraging results: Core-1 (porosity: 24.57%; air permeability: 99.56 mD; liquid permeability: 78.54 mD) yielded 52% incremental oil recovery with a polymer retention of 111 µg/g, while Core-2 (porosity: 22.13%; air permeability: 78.14 mD; liquid permeability: 54.73 mD) achieved 43% recovery with a higher polymer retention of 156 µg/g. IFT measurements showed significant reduction down to 0.096 mN/m for Core-1 and 0.112 mN/m for Core-2, while contact angle shifts toward water-wetness further validated improved displacement efficiency. Complementary XRD and FTIR analyses confirmed polymer–clay interactions with minimal structural alteration, supporting the stability of injected chemicals. Comparative injection scheme analyses and simulations reinforced the effectiveness of AP flooding under laboratory conditions. Despite potential field-scale challenges such as scaling and brine incompatibility, the findings establish AP flooding as a technically viable and effective EOR approach for mature oilfields of the Upper Assam Basin, with strong potential for pilot-scale implementation.

***Author for Correspondence**
Bhaskar Jyoti Saikia
E-mail: saikiabhaskar@dibru.ac.in

[1]Research Scholar, Department of Petroleum Engineering, Dibrugarh University Institute of Engineering and Technology, Dibrugarh University, Assam, India
[2]Assistant Professor, Department of Petroleum Engineering, Dibrugarh University Institute of Engineering and Technology, Dibrugarh University, Assam, India
[3]Associate Professor, Department of Petroleum Technology, Dibrugarh University, Assam, India
[4]Research Scholar, Department of Petroleum Technology, Dibrugarh University, Assam, India

Received Date: July 12, 2025
Accepted Date: August 30, 2025
Published Date: October 23, 2025

Citation: Joyshree Barman, Bhaskar Jyoti Saikia, Ranjan Phukan, Gauri Sankar Bora. Experimental Study on the Impact of Polymer (PAM) in Enhancing Oil Recovery in Upper Assam Basin Oil fields. Journal of Polymer & Composites. 2025; 13(6): 283–296p.

Keywords: Alkali - polymer flooding, Enhanced Oil Recovery, Non -Newtonian, Shear Thinning, Interfacial Tension

INTRODUCTION

The Upper Assam Basin in northeastern India is one of the country's most mature and extensively exploited petroleum-producing regions. With over a century of exploration and production, the oil fields in this basin are now facing terminal decline, where conventional primary and secondary recovery methods are no longer sufficient to sustain output [1]. Despite extensive waterflooding programs, a large fraction of the original oil in place (OOIP) remains unrecovered due to poor sweep efficiency, adverse mobility ratios, and reservoir heterogeneity. Chemical EOR methods, particularly AP flooding, are increasingly being

explored for such mature fields. AP flooding combines the benefits of IFT reduction through alkali and mobility control via polymer addition. The alkali component generates in situ surfactants through reaction with the crude oil's acidic components, effectively lowering IFT, while the polymer typically hydrolyzed polyacrylamide (HPAM) increases the viscosity of the displacing fluid to improve mobility control [2 - 4]. The polymer component plays a crucial role in improving areal and vertical sweep efficiencies by correcting unfavorable mobility ratios. This suppresses viscous fingering and promotes a more uniform displacement front, especially in heterogeneous formations [5]. As the mobility of a fluid increases—due to reduced viscosity or increased permeability its ability to flow also increases. Therefore, enhancing oil phase mobility is critical for improving overall recovery [3], [6]. However, successful implementation of AP flooding depends heavily on formation-specific factors. The Upper Assam Basin presents unique challenges including scaling risks, high salinity, and complex crude–brine–rock (COBR) interactions [1], [7]. Polymer degradation, adsorption, and chemical incompatibility under reservoir conditions also pose risks to performance [8], [9]. Addressing these issues requires field-specific flood design, comprehensive laboratory testing, and numerical simulation. This study evaluates the applicability of alkali–polymer (AP) flooding in the Upper Assam Basin using a combination of laboratory experiments and simulation-based approaches. Rheological measurements conducted using a coaxial cylinder viscometer confirmed that partially hydrolyzed PAM solutions exhibit non-Newtonian, shear-thinning behavior, particularly at higher polymer concentrations—an essential property for effective mobility control. Coreflooding experiments were carried out on two representative sandstone core samples to assess oil recovery performance under simulated reservoir conditions. Core Sample 1, with a porosity of 24.57% and air and liquid permeabilities of 99.56 mD and 78.54 mD respectively, achieved an incremental recovery of up to 52% of the OOIP. In comparison, Core Sample 2, with a slightly lower porosity of 22.13% and permeabilities of 78.14 mD (air) and 54.73 mD (liquid), yielded an incremental recovery of 43% OOIP. IFT was significantly reduced to 0.096 mN/m for Core-1 and 0.112 mN/m for Core-2, validating the synergistic effect of alkali and polymer in enhancing oil displacement [5], [10]. The superior performance of Core-1 can be attributed to its higher permeability, which facilitates better fluid injectivity and displacement efficiency compared to the tighter pore structure of Core-2. These findings contribute to the growing body of evidence supporting the potential of AP flooding in Indian mature reservoirs. With proper field adaptation and compatibility assessments, AP flooding can extend the productive life of declining fields such as those in the Upper Assam Basin.

MATERIALS AND METHODS

Materials Used

PAM and alkali (Na_2CO_3) were procured from Sigma-Aldrich and Loba Chemie, respectively. Crude oil was also obtained from the same formation, and its specifications are presented in Table 1. Alkali Na_2CO_3 concentration varying from 1–1.5 wt% for better IFT reduction since crude oil is having TAN $\geq$ 0.5.

In this investigation, two core samples, labeled A1 and A2, were obtained from the sandstone reservoir of the Barail Formation. Prior to conducting flooding experiments, key petrophysical parameters porosity and permeability were evaluated using a Helium Porosimeter and an Air

Table 1. Properties of crude oil.

Property	Crude oil
Sp. gravity of crude oil @ 60ºF	0.88
Acid no. of crude oil, mg KOH/g	0.75
Wax content, % (w/w)	2.1
Asphaltene content, % (w/w)	4.32
Resin content, % (w/w)	8.22
Pour point ºC	33.4

Table 2. Petrophysical properties of Core Samples.

S.N.	Core Sample	Porosity (%)	Air Permeability, mD	Liquid Permeability, mD	Area, sq cm
1	Core -A1	24.57	99.56	78.54	10.24
2	Core -A2	22.13	78.14	54.73	11.05

Table 3. Concentration of PAM (500-4500 ppm) in DW

S.N.	Amt. of DW (ml)	Amt. of PAM added (g)	Conc. of PAM solution (ppm)
1	100	0.05	500
2	100	0.15	1500
3	100	0.25	2500
4	100	0.35	3500
5	100	0.45	4500

Permeameter, respectively. Additionally, liquid permeability was derived by applying the Klinkenberg correction, extrapolating the relationship between the inverse of average pressure and measured air permeability. The physical dimensions and petrophysical characteristics of the cores are summarized in Table 2.

Methods

Sample Preparations

The PAM concentrations were prepared 500, 1500, 2500, 3500 and 4500 ppm in demineralized water (DW) was prepared Table 3.

Rheological Properties of Various Concentrations of PAM

Shear-rate dependence is a key characteristic of non-Newtonian fluids, especially time-independent types. These fluids often show Newtonian behavior at low shear rates, followed by either shear-thinning (decreasing viscosity) or shear-thickening (increasing viscosity) behavior as shear rate increases, eventually reaching a second Newtonian plateau. Most polymer solutions exhibit shear-thinning behavior. Rheological properties of the polymer solutions PAM were measured using a Brookfield R/S+ Portable Rheometer in Controlled Shear Rate (CSR) mode. Shear rates ranged from 0 to 1200 s^{-1}. The setup followed the DIN 53019/ISO 3219 coaxial cylinder system, suitable for small volumes and temperature control. Viscosity and shear stress were derived from system geometry, torque, and angular velocity. Calibration was done using a standard mineral oil at 25°C. Data was processed using Rheo 3000 software, and the rheometer was cleaned between sample runs. The mathematical principles behind the Brookfield R/S+ Rheometer (coaxial cylinder system) and how the Rheo 3000 software directly computes key rheological parameters equations (1), (2) & (3).

Shear Rate ($\dot{\gamma}$)

For a coaxial cylinder system (bob and cup):

$$\dot{\gamma} = 2\Omega Ri^2 / (Ro^2 - Ri^2) \quad (1)$$

Where;
$\dot{\gamma}$ = shear rate (s^{-1})
Ω = angular velocity of the bob (rad/s)
Ri= radius of the inner cylinder (bob)
Ro = radius of the outer cylinder (cup)

Shear Stress (τ)

$$\tau = T/2\pi LRi^2 \quad (2)$$

Where;

τ = shear stress (Pa)
T = torque (N·m)
L = length of the bob immersed in the sample (m)
Ri = radius of the inner cylinder (m)

Apparent Viscosity (η)

$$\eta = \tau / \dot{\gamma} \quad (3)$$

Where;
η = apparent viscosity (Pa·s)
τ = shear stress (Pa)
$\dot{\gamma}$ = shear rate (s^{-1})

Thermogravimetric Analysis (TGA)

TGA is essential for evaluating the thermal stability of PAM used in EOR, as the polymer must withstand elevated reservoir temperatures and salinity without losing viscosity. TGA provides critical information such as the onset of degradation, maximum decomposition temperature, and residual stability, helping to predict polymer performance under harsh reservoir conditions. It also allows comparison of different PAM formulations ensuring the selection of polymers with sufficient stability for effective mobility control and oil recovery.

IFT Measurements of Different Concentrations of Alkali with Collected Crude Oil

IFT between the crude oil and various alkali concentrations was measured using a dynamic spinning drop tensiometer. The tests evaluated the IFT reduction performance of alkali solutions at different concentrations. The capillary tube is filled with the continuous phase (alkali solution). A small droplet of crude oil is injected into the tube using a microsyringe. The tube is sealed, mounted horizontally, and rotated at controlled speed. The drop shape is captured shown in Figure 1 when diameter becomes one fourth of length, and IFT is calculated by the software using Vonnegut's equation (4).

$$\gamma = \Delta\rho\, \omega^2\, d^3 / 4 \quad (4)$$

Where;
γ = Interfacial tension (mN/m)
$\Delta\rho$ = Density difference between two fluids (g/cm^3)
ω = Angular velocity (rad/s)
d = Equatorial diameter of the drop (cm)

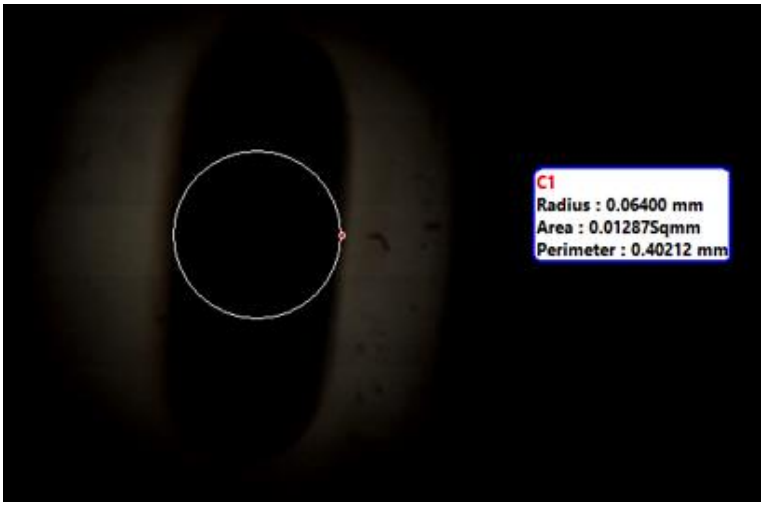

Figure 1. Oil drop shape is captured

Contact Angle Measurements

Cylindrical core discs (3.81 cm diameter, 1.2 cm thickness) were prepared using a core cutting machine, followed by end-facing and grinding to achieve uniform surfaces. The discs were cleaned in a Soxhlet apparatus, then dried in a hot-air oven at 60 °C until a constant weight was obtained. Subsequently, the dried samples were saturated with formation water for 24 hours, followed by crude oil saturating for 7 days. Formulated Alkali slugs were dispensed onto the core surfaces using a microsyringe, and contact angles were captured with a Dino-Lite digital microscope equipped with image analysis software shown in Figure 7(a)–(c).

Determination of Divalent ions (Ca^{2+}, Mg^{2+})

Total Calcium and magnesium were determined by methods FSSAI 14.035:2024 - determination of Calcium by EDTA Titrimetric Method and FSSAI 14.022:2024 - determination of Magnesium (Calculation method). Computing magnesium hardness using the formula; Magnesium hardness = [Total hardness (mg/L) − Calcium hardness (mg/L)]. Convert to magnesium concentration (as Mg^{2+}) by multiplying magnesium hardness by 0.2428 mg/L

XRD Analysis

Core samples were oven-dried at 60 °C, crushed to <75 µm, and crushed samples analyzed using a Rigaku Ultima IV X-ray diffractometer to identify clay minerals.

Polymer Retention through Adsorption

One gram of adsorbent (core sample powder A1 and A2) was added to 10 mL of adsorbate solution (PAM) and allowed to interact for 24 h in a rotospin. The mixtures were then centrifuged at 3000 rpm for 20 min. The PAM concentration was determined by measuring absorbance before and after adsorption using a UV–Vis spectrophotometer. The amount of adsorbate adsorbed onto the adsorbent, Γ(µg /g), was calculated using the mass balance equation. (5):

$$\Gamma = \frac{(C0-Ce)\times V}{M}$$

Where,

Γ = amount of adsorbate adsorbed on the adsorbent (µg/g)

C_0 = initial adsorbate concentration before adsorption (µg/mL)

C_e = equilibrium adsorbate concentration after adsorption (µg/mL)

V = volume of solution (mL)

M = mass of adsorbent (g)

FTIR Analysis

FTIR analysis was carried out using a Bruker Alpha-E spectrometer to record spectra of the samples before and after PAM slug flooding.

Coreflooding

Core flooding experiments were conducted using reservoir core plugs of 1.5-inch diameter and 4.2-inch length. The core samples were cleaned using Soxhlet extraction followed by Ultrasonic cleaner to remove residual oil and salts, then dried, weighed, and characterized for petrophysical properties. The selectivity of the solvents is influenced by the clay mineral composition of the core. To ensure standardized preparation, core samples were conditioned in a humidity oven maintained at 63°C and 40% relative humidity, following the guidelines outlined in API-RP-40 (1998): Recommended Practices for Core Analysis [11]. The total heating duration was approximately 42 hours. At regular intervals, the partially dried core plugs were removed from the oven and weighed repeatedly until a constant mass was achieved, indicating complete moisture removal. After baseline oil recovery through brine injection, an alkali solution was injected, followed by polymer injection at a controlled rate to enhance oil recovery. An optional post-flush with brine was carried out to assess polymer

retention. Throughout the experiment, oil and water production, pressure drop, polymer breakthrough, and effluent concentration were monitored to calculate recovery factors, incremental oil recovery, resistance factor, and residual resistance factor.

RESULTS AND DISCUSSION

Rheological Behaviours of Various Concentrations 500, 1500, 2500, 3500 and 4500 ppm of PAM

Figure 2 showed the rheological behaviour of fluids under definite shear stress and shear rate. PAM, a water-soluble polymer widely used in EOR, exhibits non-Newtonian shear-thinning (pseudoplastic) behavior, a key characteristic that enhances its performance during injection and displacement processes in porous media.

Figure 3 illustrates the shear-rate-dependent behavior of PAM at concentrations ranging from 500 to 4500 ppm in distilled water. At lower concentrations (500, 1500, 2500, and 3500 ppm), PAM solutions exhibited shear-thickening behavior, where shear stress increased exponentially with shear rate indicative of dilation or solid-like suspension behavior [12, 13]. In contrast, the 4500 ppm PAM solution showed shear-thinning behavior, where shear stress increased with a negative slope, as described by [14]. Both trends confirm the non-Newtonian nature of PAM, where shear stress is not linearly proportional to shear rate. Shear-thickening fluids behave like solids under stress due to flocculation, while shear-thinning fluids show reduced viscosity with increasing shear rate, often misinterpreted as Newtonian at extreme rates [15]. Reservoir suitability depends on flow behavior: shear-thickening PAM is preferred for homogeneous reservoirs, while shear-thinning PAM is more

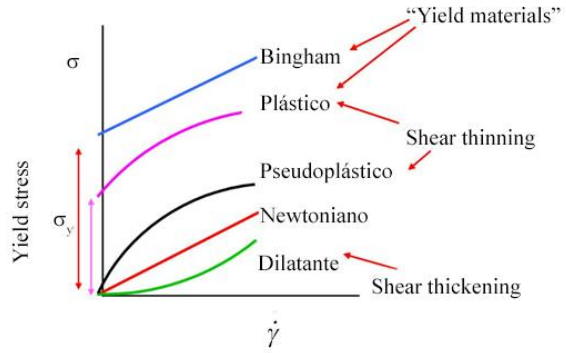

Figure 2. Rheological properties of fluids definite shear stress and shear rate

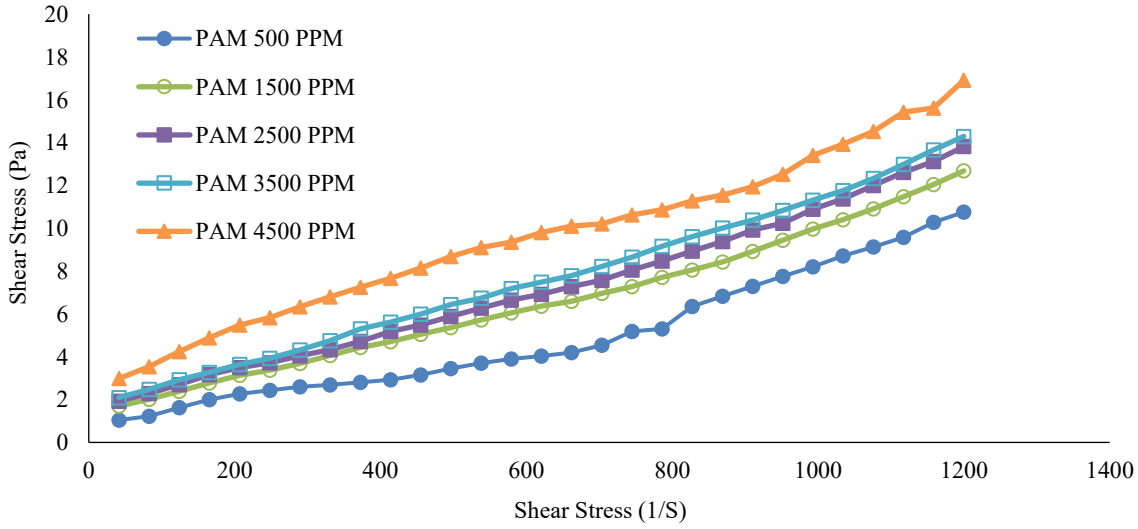

Figure 3. Shear stress (Pa) vs. Shear Rate (s^{-1}) of various concentrations of PAM

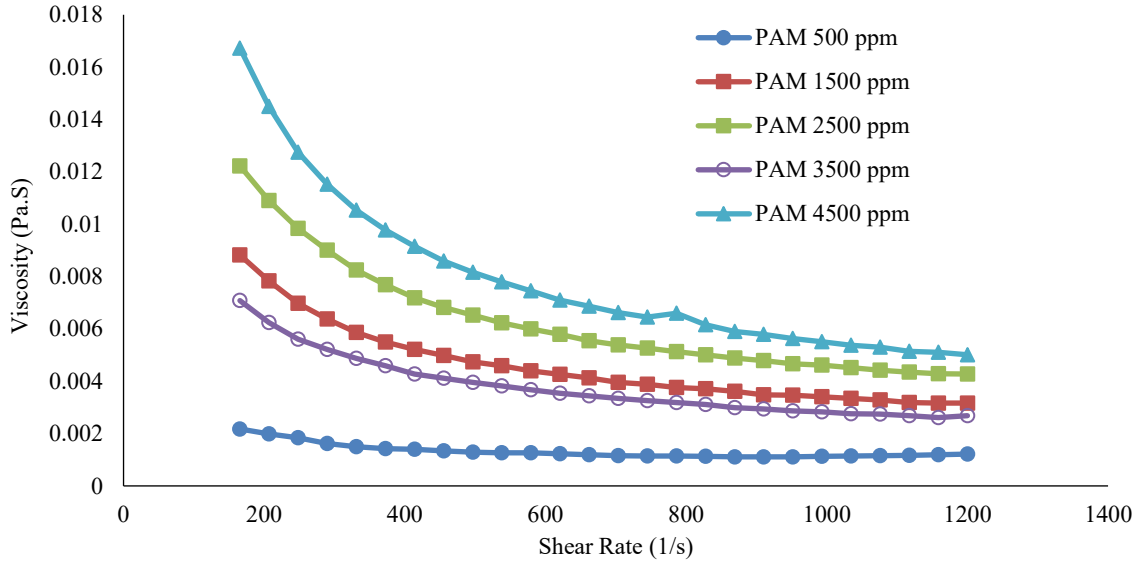

Figure 4. Viscosity (Pa.s) vs. Shear Rate (s^{-1}) of various concentrations of PAM

effective in heterogeneous formations. Apparent viscosity versus shear rate plots in Figure 4 further confirm the non-Newtonian, yield-stress-dependent flow of PAM solutions. At low shear rates, PAM solutions show relatively constant viscosity referred to as the lower Newtonian plateau. As shear rate increases, viscosity decreases, due to alignment of polymer chains in the direction of flow, reducing internal resistance. At high shear rates, viscosity tends to level off again, approaching the upper Newtonian plateau. This shear-thinning property is advantageous during core flooding: High viscosity in porous media improves sweep efficiency. Lower viscosity near the wellbore helps reduce injection pressure requirements, improving injectivity. As observed from Figures 3 and 4, the 4500 ppm PAM solution exhibited shear-thinning behavior, where viscosity decreases with increasing shear rate. This makes it suitable for injection into heterogeneous reservoirs, as shear-thinning polymers can better navigate pore throat variations and improve sweep efficiency. Therefore, 4500 ppm PAM was selected for core flooding experiments.

TGA Analysis

Figure 5 shows the TGA curves of PAM1, PAM 2, PAM3 and PAM4 (4500, 3500 ppm, 2500 ppm and 1500 ppm) show an initial minor weight loss below 150 °C due to moisture evaporation, followed by a major degradation step between 300–500 °C related to backbone decomposition. PAM1 retained the highest residue (~52% at 700 °C), indicating superior thermal stability, while PAM4 left the lowest (~32%), suggesting weaker resistance to high temperatures. These differences highlight the variation in thermal endurance among the samples, which is important for selecting suitable PAM formulations for EOR applications. PAM1 showed best thermal stability.

IFT Experiments

The crude oil used in this study has a TAN of 0.75 mg KOH/g, which is considered relatively high and favorable for alkali flooding. A high TAN indicates the presence of sufficient naphthenic acids in the crude, allowing effective reaction with injected alkali (Na_2CO_3) to form in-situ surfactants (soaps), as shown in Equation (5):

$$R\text{-}COOH + NaOH \rightarrow R\text{-}COONa + H_2O \quad (5)$$

This in-situ soap formation significantly reduces the interfacial tension (IFT) between oil and water, enhancing oil mobilization and recovery. Industry literature suggests that crude oils with TAN values above 0.3 mg KOH/g are typically suitable for alkali flooding. As shown in Figure 6, IFT decreases with increasing Na_2CO_3 concentration, further supporting the effectiveness of this approach.

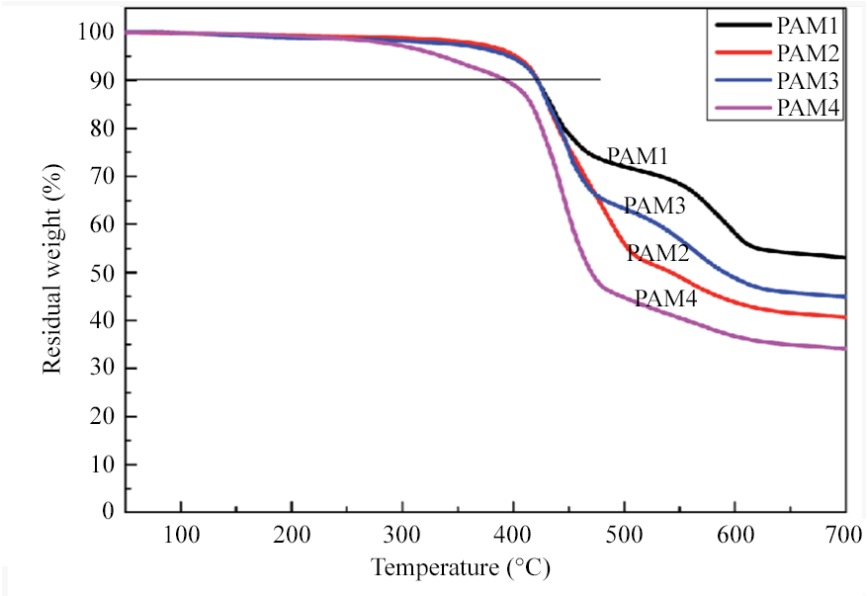

Figure 5. TGA curves of different concentrations of PAM

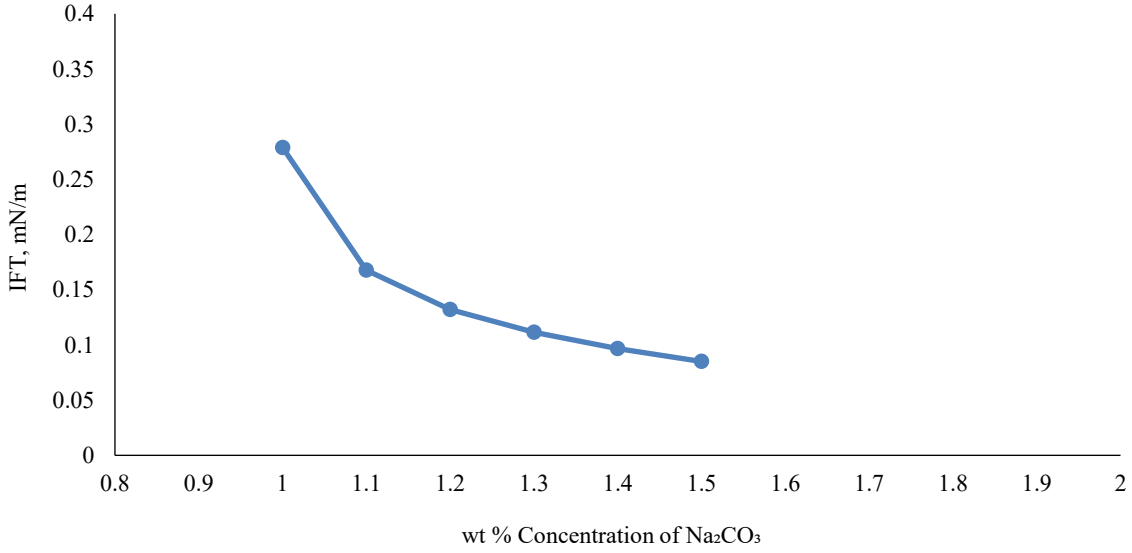

Figure 6. IFT vs conc. of Alkali Na_2CO_3

However, excessive alkali concentrations can lead to undesirable effects such as scaling due to precipitation with divalent ions (Ca^{2+}, Mg^{2+}), stable emulsion formation, polymer degradation at high pH, and equipment corrosion [16, 17]. These effects not only hinder recovery but also increase operational cost, complexity, and environmental risks. Therefore, it is essential to select an optimum alkali concentration that effectively reduces IFT without causing formation damage or operational challenges. Based on industry practice and performance balance, Na_2CO_3 concentrations in the range of 0.5–1.5 wt% are typically recommended [18, 19]. In this study, a middle-range concentration of 1.1 wt% Na_2CO_3 was selected for alkali flooding to ensure both efficiency and operational safety.

Contact Angle Measurements Results

Contact angle measurements for 1.1 wt% Na_2CO_3 on Core-A1 and Core-A2 (Figure 7(a)–(c)) further confirm that the observed IFT reduction is due to the in-situ formation of sodium naphthenates, generated through the reaction between crude oil acids (TAN) and Na_2CO_3, resulting in effective in-situ surfactants [20, 21]. In Figure 7(a), where distilled water was used, the contact angle

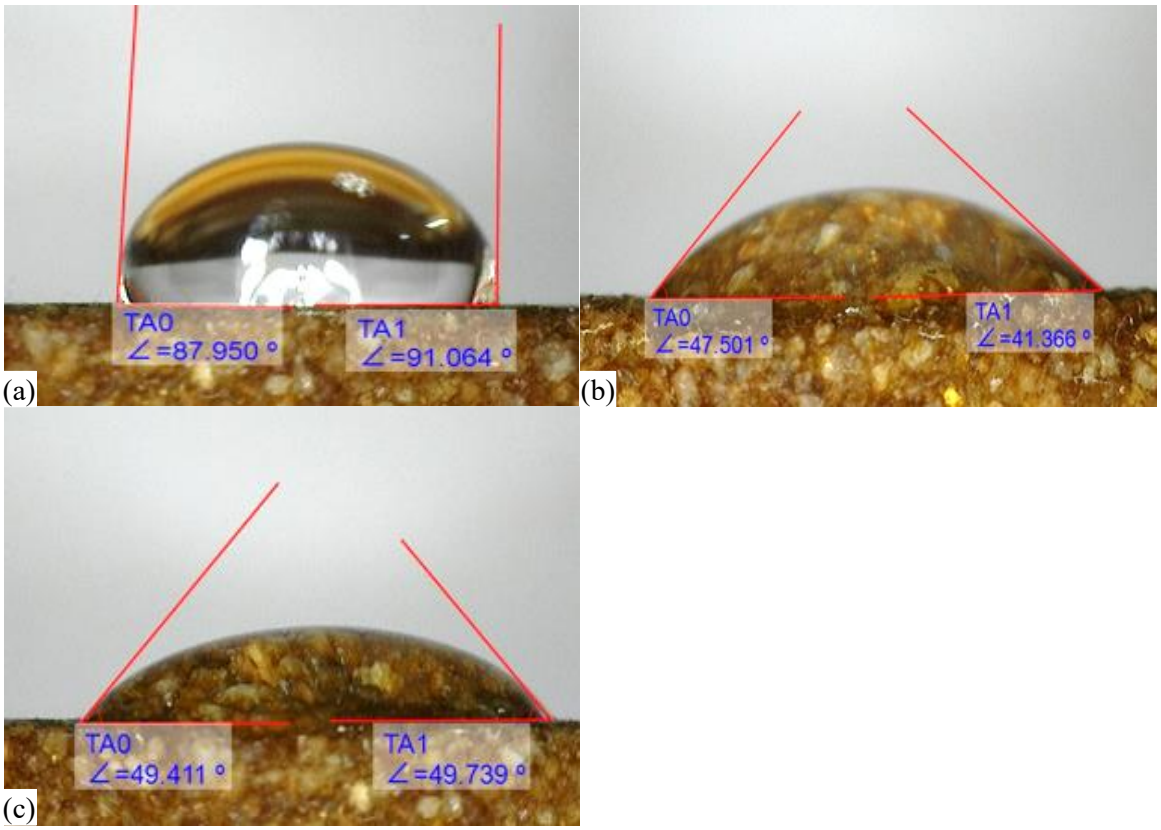

Figure 7. (a) Contact angle DW, (b) 1.1 wt% Na_2CO_3 on Core-A1, (c) 1.1 wt% Na_2CO_3 on Core-A2

Table 4. Divalent ions (Ca^{2+}, Mg^{2+}) of field brine quantifications before and after flooding

S.N.	Core sample	Before flooding		After flooding	
		Ca^{2+} (mg/L)	*Mg^{2+} (mg/L)*	*Ca^{2+} (mg/L)*	*Mg^{2+} (mg/L)*
1	Core - A1	0.8	18.54	0.5	13.45
2	Core - A2	1.2	19.11	0.71	15.32

was relatively high, indicating lower wettability and reduced miscibility between oil and water. Upon the addition of alkali, the contact angle decreased significantly (Figure 7(b) and (c)), reflecting a shift towards a more water-wet surface condition, which is favorable for enhanced oil displacement.

Divalent ions (Ca^{2+}, Mg^{2+}) Quantifications

Total hardness and calcium were measured by EDTA titration following FSSAI protocols. Calcium was determined using FSSAI 14.035:2024 (EDTA titrimetric method) after appropriate buffering and masking steps. Total hardness (as $CaCO_3$) was determined by standard EDTA titration (FSSAI methodology). Magnesium hardness was calculated using FSSAI 14.022:2024 (calculation method):

Magnesium hardness (mg/L as $CaCO_3$ =Total hardness (mg/L as $CaCO_3$) − Calcium hardness (mg/Las $CaCO_3$). Magnesium concentration (mg/L as Mg^{2+}) was obtained from magnesium hardness using the conversion factor: Mg^{2+} (mg/L) = Magnesium hardness (mg/L as $CaCO_3$) × 0.2428

All titrations used certified EDTA standard solutions and Eriochrome Black T/Calamite indicators as specified in the FSSAI methods. Table 4 shows the Na_2CO_3 reacts with dissolved Ca^{2+} and Mg^{2+} to form insoluble precipitates such as $CaCO_3$, $MgCO_3$, or mixed carbonates. These precipitates drop out of solution, so the measured Ca^{2+} and Mg^{2+} in the produced brine will be lower than before flooding.

XRD Clay Minerals Identification and Analysis

Core-A1 and Core-A2 are both quartz-dominated sandstones (strong peak at ~26° 2θ), but they differ in their clay and feldspar content: Core-A1 shows quartz with minor kaolinite and illite peaks, whereas Core-A2 displays relatively stronger clay (kaolinite, illite) signals together with more prominent feldspar/anorthite reflections as shown in Figure 8(a) and (b). In practical terms, the higher clay content in Core-A2 means greater potential for PAM adsorption, which can reduce effective polymer concentration in the pore fluid, alter wettability, and increase the risk of permeability loss or fines mobilization. For EOR, this suggests that polymer formulation and injection strategy should be adjusted in clay-rich formations to minimize polymer loss and maintain efficiency.

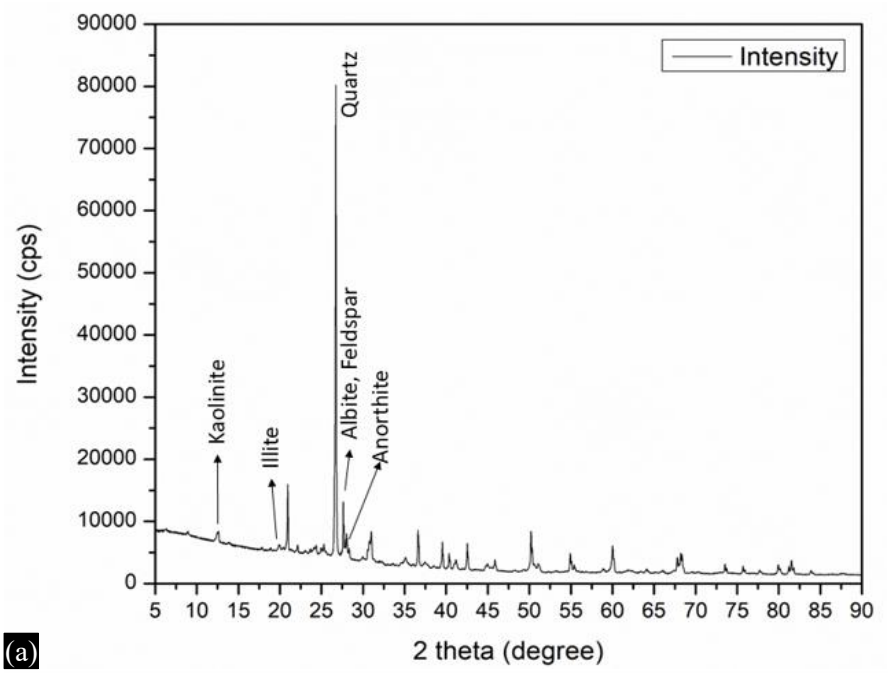

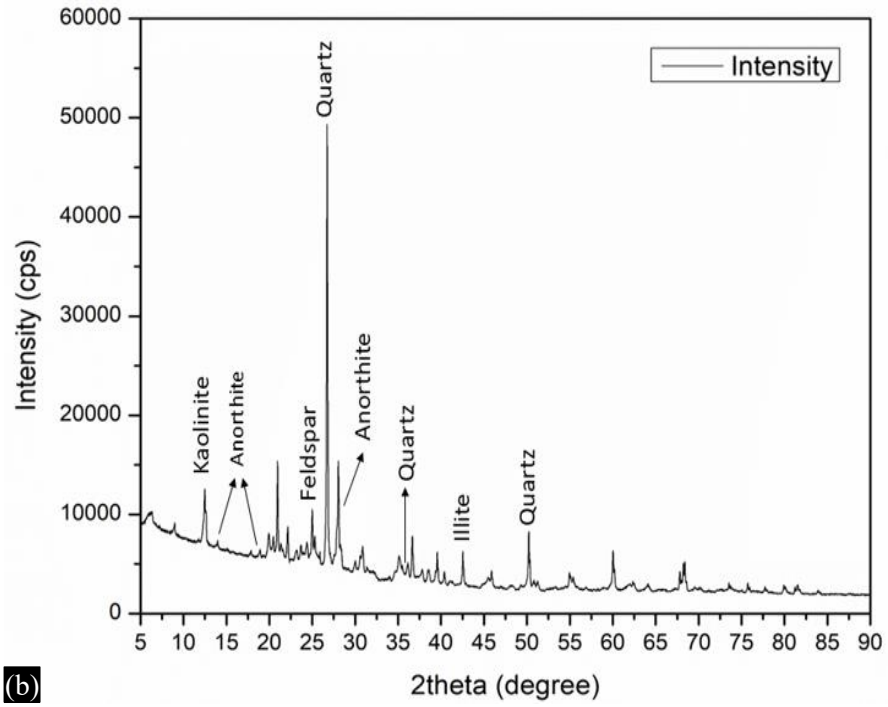

Figure 8. (a) XRD Clay identification Core-A1, (b) XRD Clay identification Core-A2

Polymer Retention and Coreflooding Experiments Results

All flooding experiments were carried out at a reservoir-simulated temperature of 70°C. Table 5 presents the connate water saturation (Swc) values corresponding to pore volume and ageing duration. The core plugs were aged for a period ranging from 14 to 27 days within a core holder under a confining pressure of 200 psi, allowing sufficient time for establishing COBR equilibrium.

Core flooding experiments have been performed for the saturated 02 nos. core samples in 04 different core flooding methods. The purpose is to check the efficency of the polymer with alkali in enhancing oil recovery. The incremental oil recovery has been calculated in terms of OOIP. The oil recovery results are tabulated in Table 6. The AP flooding case demonstrated the highest recovery, lowest IFT, and reduced polymer retention due to favourable wettability for the core -A1 Compared to A2 in Table 6.

Core-A1, which had a porosity of 24.57% and permeabilities of 99.56 mD (air) and 78.54 mD (liquid), yielded an incremental recovery of 52% of the OOIP. In contrast, Core-A2, with slightly lower porosity (22.13%) and permeabilities of 78.14 mD (air) and 54.73 mD (liquid), showed a recovery of 43% OOIP. The higher recovery in Core-A1 can be attributed to its greater permeability and pore connectivity, which facilitated more uniform fluid front advancement and efficient sweep. Enhanced injectivity and reduced resistance to flow allowed the alkali–polymer slug to access and mobilize residual oil trapped in pore throats more effectively. Conversely, the relatively lower permeability of Core-A2 likely increased resistance to flow and restricted polymer propagation, resulting in comparatively reduced sweep efficiency. These results emphasize the importance of reservoir rock properties, particularly permeability, in determining the success of chemical EOR processes like AP flooding. Higher permeability zones are more receptive to polymer injections and provide better conformance control, which is critical in heterogeneous formations [22].

FTIR analysis

The FTIR spectra of PAM before and after flooding show the typical functional groups of the polymer, with broad N–H stretching vibrations around 3200–3400 cm^{-1}, C–H stretching near 2920 cm^{-1}, and prominent amide I (C=O stretching) and amide II (N–H bending) bands at ~1650 and ~1600 cm^{-1}, confirming the characteristic structure of polyacrylamide (Figure 9(a) and (b)).

After flooding, these functional groups are still evident, indicating that the main polymer backbone remains intact under reservoir conditions. However, slight shifts in peak position along with reduced intensity, particularly in the N–H and C=O regions, suggest that some of these groups are involved in interactions with formation minerals and brine. This behavior points to adsorption of PAM molecules

Table 5. Connate Water Saturation, (Swc) of the core samples

S.N.	Core sample	Pore volume	Aging time, days	Connate water saturation, (Swc)
1	Core -A1	14.21 cc	15	27.51%
2	Core - A2	13.89 cc	27	28.42%

Table 6. Coreflooding results, IFT and Polymer retention of Core -A1 and Core-A2

Flooding method	Concentration	Incremental recovery, (%)		IFT (mN/m)		Polymer retention (µg/g)	
		Core-A1	*Core-A2*	*Core-A1*	*Core-A2*	*Core-A1*	*Core-A2*
Water flooding		25	23				
Polymer only	4500 ppm	37	32			198	245
Alkali only	1.1 wt% Na_2CO_3	43	39	0.1677	0.234		
Alkali Polymer flooding	1.1 wt% Na_2CO_3 + 4500 ppm PAM	52	43	0.096	0.112	111	156

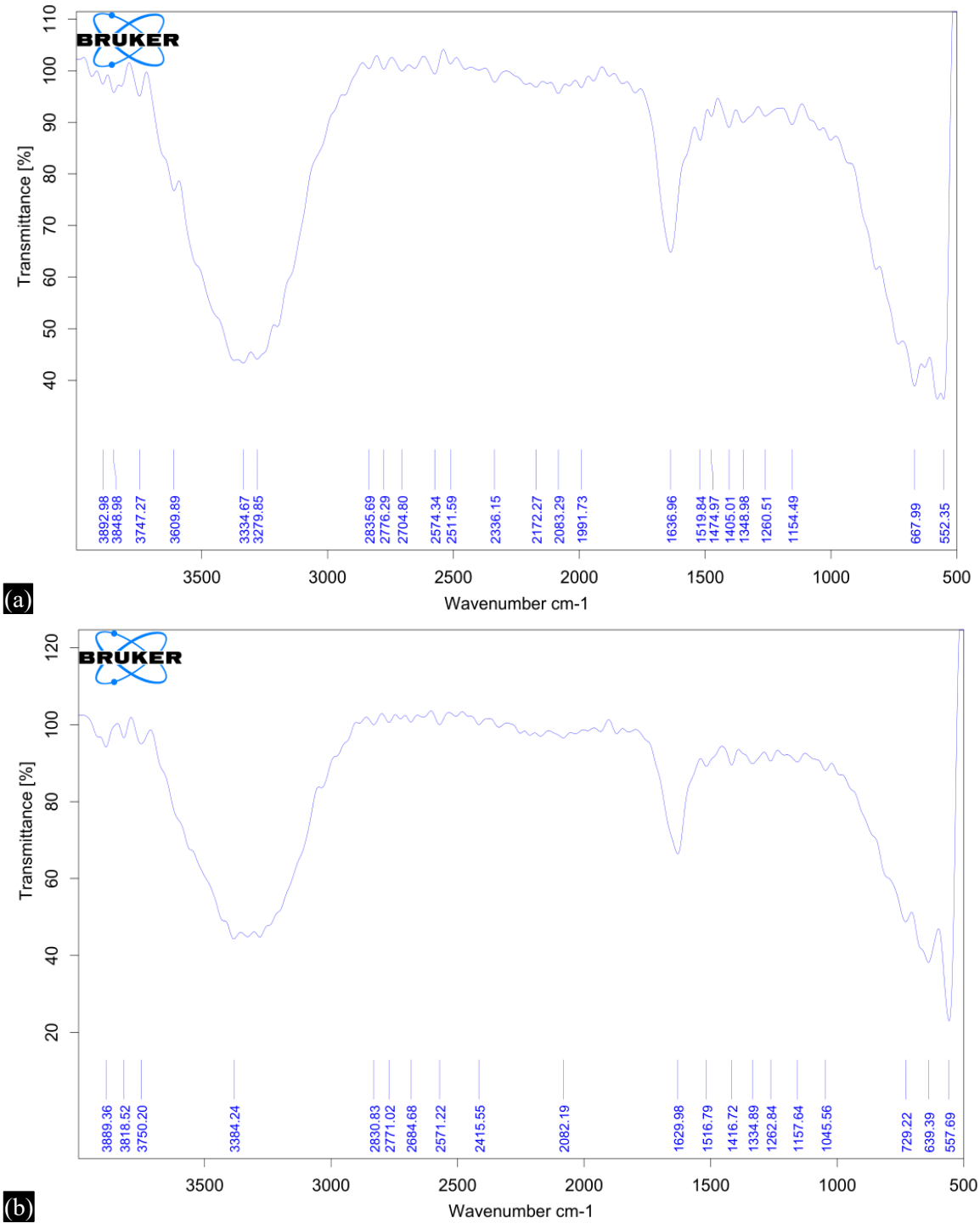

Figure 9. (a) FTIR 4500 ppm PAM before flooding, (b) FTIR 4500 ppm PAM after flooding

on clay and mineral surfaces within the rock, leading to partial polymer loss. Such interactions are important in EOR, as they influence polymer efficiency, solution viscosity, and overall oil recovery performance [23].

CONCLUSIONS

AP flooding presents a promising EOR technique for the mature reservoirs of the Upper Assam Basin, as demonstrated through laboratory experiments and simulation studies. The major findings are summarized below:

1. *Rheological behavior:* PAM solutions displayed non-Newtonian, shear-thinning behavior as measured by a coaxial cylinder viscometer. This ensures better injectivity near the wellbore while maintaining higher viscosity deeper in the reservoir, improving sweep efficiency and mobility control.
2. *Thermal stability:* Higher-concentration PAM (4500 ppm) showed superior thermal stability compared to lower concentrations (1500 ppm), confirming its suitability under elevated reservoir temperatures.
3. *Incremental oil recovery:*
   i. Core A1 (porosity: 24.57%; permeability: 99.56 mD air, 78.54 mD liquid) achieved 52% incremental oil recovery (OOIP).
   ii. Core A2 (porosity: 22.13%; permeability: 78.14 mD air, 54.73 mD liquid) achieved 43% incremental oil recovery.
   iii. The higher permeability of Core A1 led to more effective displacement and sweep efficiency than Core A2.
4. *IFT reduction:* AP flooding significantly reduced IFT, reaching 0.096 mN/m in Core A1 and 0.112 mN/m in Core A2. This demonstrates the synergistic role of alkali in generating in-situ surfactants and mobilizing residual oil.
5. *Effect of rock properties:* XRD analysis confirmed clay minerals in both cores, with Core A2 showing higher clay content, leading to greater polymer adsorption and reduced efficiency. These results highlight that porosity, permeability, and clay content critically influence AP flooding performance.
6. *FTIR analysis:* FTIR spectra of PAM before and after flooding confirmed that the main functional groups (–$CONH_2$ and –CH_2) remained intact. However, minor shifts indicated polymer–mineral interactions, explaining partial polymer retention in the reservoir rock.
7. *Overall applicability:*
   i. AP flooding is validated as a technically viable and effective EOR method for mature oilfields in the Upper Assam Basin.
   ii. Reservoir heterogeneity (porosity, permeability, clay content) must be carefully considered when designing polymer formulations and injection strategies.
   iii. Further pilot-scale field trials are recommended to confirm laboratory and simulation results before full-scale implementation.

REFERENCES

1. Sheng J.J. Modern chemical enhanced oil recovery: Theory and practice. Gulf Professional Publishing. 2023; 2nd ed., Houston, TX, USA.
2. Lake L.W. Enhanced oil recovery. Society of Petroleum Engineers. 2014; Richardson, TX, USA.
3. Thomas S. Current status of chemical EOR and future prospects. Oil Gas Sci Technol – Rev IFP Energies nouvelles. 2022; 77(4): 201–14.
4. Alvarado V, Manrique E. Enhanced oil recovery: An update review. Energies. 2010; 3(9): 1529–75.
5. Singh M, Islam A. Field-scale simulation of alkali-polymer flooding in mature Indian oilfields. SPE J. 2025; 30(2): 213–25.
6. Zolotukhin A, Ursin J.R. Application of polymer-based EOR in low-permeability reservoirs: Challenges and recent advances. J Pet Explor Prod Technol. 2024; 14(1): 89–102.
7. Alagic A, Skauge S. Combined low salinity brine and polymer flooding: A review. Energy Fuels. 2023; 24: 5657–70.
8. Austad T. Water-based EOR in carbonates and sandstones: New chemical understanding of the EOR potential using smart water. In: Enhanced Oil Recovery Field Case Studies. Elsevier. 2013.
9. Sheng M. Modern chemical enhanced oil recovery. Gulf Professional Publishing. 2010.
10. Liu Y, et al. Enhanced oil recovery by alkali-polymer flooding in a sandstone reservoir. SPE Reserv Eval Eng. 2018; 21: 956–67.

11. American Petroleum Institute. Recommended practices for core analysis. API. 1998; 2nd ed.: 2/14–18, February.
12. Jha B, Mandal S. Application of polymer flooding in Indian oilfields: A case study of Ankleshwar field. J Pet Eng. 2020; Article ID 7890134.
13. Kamath S.R, Patil R. Chemical EOR evaluation for Indian reservoirs. Petroleum Research. 2019; 4(1): 32–9.
14. Zitha P, Torsæter L. Alkaline–polymer flooding in low permeability reservoirs. J Pet Sci Eng. 2015; 129: 80–9.
15. Islam M.R, et al. Performance evaluation of EOR techniques in Assam oil fields. Indian J Pet Geol. 2022; 29(2): 61–72.
16. ONGC. Enhanced oil recovery potential in Assam–Arakan basin. Internal Report, Oil and Natural Gas Corporation. 2020.
17. Nasr-El-Din M, et al. Use of sodium carbonate in chemical flooding: Advantages and limitations. SPE Paper 113910, presented at SPE Conference. 2008.
18. Bernard G.G. Effect of floodwater salinity on recovery of oil from cores containing clay. 38th Annual California Regional Meeting, SPE AIME, Los Angeles, CA. 1967; 26–7 October, SPE 1725.
19. A. A. Olajire, "Application of Polymers for Chemical Enhanced Oil Recovery: A Review," Polymers, vol. 14, no. 7, p. 1433, 2022.
20. Y. Wang, Y. Liu, J. Han, Z. Du, and X. Zhao, "Review on Chemical Enhanced Oil Recovery Using Polymer Flooding: Fundamentals, Experimental and Numerical Simulation," Petroleum Research, vol. 5, no. 1, pp. 25–36, 2020.
21. M. S. AlSofi, A. Blunt, and R. H. Valvatne, "The Impact of Rheology on Viscous Oil Displacement by Polymers Analyzed by Pore-Scale Network Modelling," Polymers, vol. 13, no. 8, p. 1259, 2021.
22. M. I. A. Mutalib, R. A. Rahman, M. F. M. Din, N. A. Zakaria, and Z. Harun, "Evaluation of Polymeric Materials for Chemical Enhanced Oil Recovery," Processes, vol. 8, no. 3, p. 361, 2020.
23. J. Sheng, "Critical Review of Alkaline–Polymer Flooding," Journal of Petroleum Exploration and Production Technology, vol. 7, no. 1, pp. 147–158, 2017

